Pergamon

Int. J. Solids Structures Vol. 32, No. 10, pp. 1331–1347, 1995

0020–7683/95 $9.50 + .00

0020–7683(94)00206–1

STABILITY AND OPTIMAL DESIGN OF LAMINATED PLATES WITH INTERNAL SUPPORTS

SERGE ABRATE
Department of Mechanical and Aerospace Engineering and Engineering Mechanics, University of Missouri at Rolla, Rolla, MO 65401, U.S.A.

(*Received* 10 *May* 1994; *in revised form* 20 *August* 1994)

Abstract—The stability of symmetrically laminated rectangular composite plates with internal line supports and point supports is analyzed using the Rayleigh–Ritz method. Polynomial approximation functions are selected to satisfy both the boundary conditions along the edges and the zero displacement constraint along any number of internal line supports. Point supports are introduced using the Lagrange multiplier technique. The elastic and geometric stiffness matrices are obtained exactly, and the plate constitutive equations are expressed in terms of four lamination parameters to describe all symmetric laminates regardless of the number of plies. An exact solution for simply supported plates with equal length spans and no bending–twisting coupling is used to check the accuracy of the model. Extensive results are presented, and the effect of the number of plies, plate aspect ratio, material properties and lay-up are examined in detail. The lowest critical load is shown to be maximum when a symmetric angle-ply laminate is used, and the influence of the material properties on the optimal lay-up is small.

The model developed is used to find which lay-ups maximize the first critical load for rectangular plates with internal supports and any combination of boundary conditions along the edges. For all the cases examined, the optimal design is a symmetric angle-ply laminate, and the optimal design is relatively unaffected by the elastic properties of the material.

INTRODUCTION

Multi-span plates are used in many applications, and the prediction of their dynamic response often requires study of their stability. The natural frequencies of isotropic rectangular plates continuous over intermediate line supports were determined by Azimi *et al.* (1984) using the receptance method. Kim and Dickinson (1987) and Liew and Lam (1991) used the Rayleigh–Ritz method and presented extensive results for isotropic plates. Abrate and Foster (1994) studied the free vibrations of laminated composite plates with internal line supports using the Rayleigh–Ritz method. Further references to earlier studies on vibrations of multi-span plates are given by Kim and Dickinson (1987) and Liew and Lam (1991). An overview of buckling of composite plates presented recently by Leissa (1987) showed that the stability of multi-span plates had not been investigated.

In this paper, a general approach is presented for analyzing rectangular composite plates with arbitrary boundary conditions along the edges and any number of intermediate line supports which can be arbitrarily located. A variational formulation is developed, and using the Rayleigh–Ritz method with simple polynomial approximation functions, a variational approximation that can easily accommodate various boundary conditions and internal line supports is obtained. Elastic and geometric stiffness matrices are evaluated exactly. Symmetrically laminated composite plates are considered, and the bending rigidities are expressed in terms of four invariants that account for the effect of lay-up regardless of the number of plies in the laminate. When searching for lay-ups that will maximize the lowest critical load, only four design variables need be considered for symmetric laminates. This number is reduced to two for laminates with more than six plies as the bending–twisting coupling becomes negligible.

FORMULATION

The transverse motion of plates subjected to initial in-plane forces N_x^o, N_y^o, and N_{xy}^o is governed by the equation (Vinson and Sierakowski, 1986)

$$M_{x,xx}+2M_{xy,xy}+M_{y,yy}+N_x^o w_{,xx}+N_y^o w_{,yy}+2N_{xy}^o w_{,xy}=0 \tag{1}$$

where M_x, M_{xy}, and M_y are the moment resultants, and w is the transverse displacement of the plate. The variational formulation of the problem defined by eqn (1) and appropriate boundary conditions are obtained by multiplying eqn (1) by a test function v and integrating over Ω, the domain occupied by the plate.

$$-\int_\Omega \{\bar{\kappa}\}^T\{M\}\,d\Omega+\int_\Omega [N_x^o v_{,x}w_{,x}+N_y^o v_{,y}w_{,y}+N_{xy}^o (v_{,x}w_{,y}+v_{,y}w_{,x})]\,d\Omega$$
$$-\int_\Gamma v\,[N_x^o w_{,x}n_x+N_y^o w_{,y}n_y+N_{xy}^o(w_{,y}n_x+w_{,x}n_y)]\,d\Gamma$$
$$=\int_\Gamma vQ_n\,d\Gamma-\int_\Gamma (v_{,n}M_n+v_{,t}M_{nt})\,d\Gamma \tag{2}$$

where Q_n is the transverse shear force acting on the boundary Γ with normal and tangent vectors $\bar{n}$ and $\bar{t}$, respectively. M_n and M_{nt} are the moment resultants acting on that boundary and

$$\{\bar{\kappa}\}^T=[-v_{,xx},-v_{,yy},-2v_{,xy}]. \tag{3}$$

For a generally laminated plate, the transverse and in-plane deformations are coupled together [Vinson and Sierakowski (1986)], but for symmetrically laminated plates the moment resultants are related to the plate curvature by

$$\begin{Bmatrix} M_x \\ M_y \\ M_{xy} \end{Bmatrix}=\begin{bmatrix} D_{11} & D_{12} & D_{16} \\ D_{12} & D_{22} & D_{26} \\ D_{16} & D_{26} & D_{66} \end{bmatrix}\begin{Bmatrix} w_{,xx} \\ w_{,yy} \\ w_{,xy} \end{Bmatrix} \tag{4}$$

or

$$\{M\}=[D]\{\kappa\}. \tag{5}$$

The D_{ij}s are the bending rigidities of the plate and, with the classical plate theory, the curvatures are defined as

$$\{\kappa\}^T=[-w_{,xx},-w_{,yy},-2w_{,xy}]. \tag{6}$$

For cases where either the displacements $(v, v_{,n}, v_{,t})$ are fixed or the prescribed forces or moments are zero, we obtain the variational eigenvalue problem

$$\int_\Omega \{\bar{\kappa}\}^T[D]\{\kappa\}\,d\Omega=\int_\Omega [N_x^o v_{,x}w_{,x}+N_y^o v_{,y}w_{,y}+N_{xy}^o (v_{,x}w_{,y}+v_{,y}w_{,x})]\,d\Omega$$
$$-\int_\Gamma v[N_x^o w_{,x}n_x+N_y^o w_{,y}n_y+N_{xy}^o(w_{,y}n_x+w_{,x}n_y)]\,d\Gamma. \tag{7}$$

When the edges of the plate are supported so that $w=0$, the test function v must also be zero along the edges, and the line integral in eqn (7) vanishes. With the Rayleigh–Ritz approximation method, an N-term approximation of the transverse displacement is taken as

$$w_N = \sum_{j=1}^{N} c_j \phi_j(x, y) \tag{8}$$

where the approximation functions $\phi_j(x, y)$ must satisfy the essential (or displacement) boundary conditions of the problem [Reddy (1984)]. Taking $v = \phi_i$, we get the eigenvalue problem

$$[K]\{c_j\} = (N_x^o[S^1] + N_y^o[S^2] + N_{xy}^o[S^3])\{c_j\} \tag{9}$$

where

$$K_{ij} = \int_\Omega \{D_{11}\phi_{i,xx}\phi_{j,xx} + D_{22}\phi_{i,yy}\phi_{j,yy} + D_{12}(\phi_{i,xx}\phi_{j,yy} + \phi_{i,yy}\phi_{j,xx}) + 4D_{66}\phi_{i,xy}\phi_{i,xy} + 2D_{16}(\phi_{i,xx}\phi_{j,xy} + \phi_{i,xy}\phi_{j,xx}) + 2D_{26}(\phi_{i,yy}\phi_{j,xy} + \phi_{i,xy}\phi_{j,yy})\}\, d\Omega \tag{10}$$

$$S_{ij}^1 = \int_\Omega \phi_{i,x}\phi_{j,x}\, d\Omega, \quad S_{ij}^2 = \int_\Omega \phi_{i,y}\phi_{j,y}\, d\Omega$$

$$S_{ij}^3 = \int_\Omega (\phi_{i,x}\phi_{j,y} + \phi_{i,y}\phi_{j,x})\, d\Omega. \tag{11a, b}$$

$[K]$ is called the elastic stiffness matrix and $N_x^o[S^1] + N_y^o[S^2] + N_{xy}^o[S^3]$ is the generalized geometric stiffness matrix. Once a set of approximation functions has been selected, the elastic and geometric stiffness matrices are evaluated exactly using the approach described in Abrate and Foster (1994). The eigenvalue problem [eqn (9)] is solved to obtain the critical loads and the corresponding mode shapes using the inverse iteration method.

APPROXIMATION FUNCTIONS

For a rectangular plate extending from 0 to a in the x-direction, and 0 to b in the y-direction, with p line supports parallel to the x-axis and q line supports parallel to the y-axis, the approximation functions are taken as

$$\Phi_1(x, y) = x^i y^m \prod_{k=1}^{p} (x - x_k) \prod_{l=1}^{q} (y - y_l) \tag{12}$$

with i starting from $i_o = 0$, 1 or 2 for free, simply supported or clamped support conditions along the edge $x = 0$. Similarly, j starts from $j_o = 0$, 1, or 2 depending on whether the edge $y = 0$ is free, simply supported, or clamped. The zero displacement constraint along straight lines parallel to the y axis and located at $x = x_k$ is enforced by the $(x - x_k)$ terms in eqn (12). Similarly, the $(y - y_l)$ terms in eqn 12 enforce zero displacement constraints along lines parallel to the x axis at various locations y_l. Support conditions along the edges $x = a$ and $y = b$ are modeled by introducing line supports along those edges when necessary.

In the displacement approximation [eqn (8)], N terms are taken so that there will be N functions ϕ_i defined by eqn 12 with $i_o \leqslant i \leqslant i_o + n_x - 1$, $j_o \leqslant j \leqslant j_0 + n_y - 1$ so that $N = n_x \cdot n_y$. The solution is then called an $n_x \times n_y$ approximation.

CONSTITUTIVE EQUATIONS

For laminated plates with orthotropic layers, the fiber orientation in each ply, the ply thicknesses, the number of plies and the material properties affect the rigidity of the plate. With the stiffness invariant formulation that is used here, the effects of the lamination scheme, laminate thickness, and material properties are investigated using a minimum number of design variables. For generally laminated plates, a maximum of 12 parameters

is needed in order to describe all possible lay-ups regardless of the number of plies. For symmetric laminates, only four such parameters are needed, and the bending rigidities in eqn (4) can be written as

$$\begin{Bmatrix} D_{11} \\ D_{22} \\ D_{12} \\ D_{66} \\ D_{16} \\ D_{26} \end{Bmatrix} = \frac{h^3}{12} \begin{bmatrix} 1 & \zeta_9 & \zeta_{10} & 0 & 0 \\ 1 & -\zeta_9 & \zeta_{10} & 0 & 0 \\ 0 & 0 & -\zeta_{10} & 1 & 0 \\ 0 & 0 & -\zeta_{10} & 0 & 1 \\ 0 & +\zeta_{11}/2 & \zeta_{12} & 0 & 0 \\ 0 & +\zeta_{11}/2 & -\zeta_{12} & 0 & 0 \end{bmatrix} \begin{Bmatrix} U_1 \\ U_2 \\ U_3 \\ U_4 \\ U_5 \end{Bmatrix} \tag{13}$$

where h is the laminate thickness. The stiffness invariants are defined as

$$\begin{aligned} U_1 &= [Q_{11}+2(Q_{12}+2Q_{66})+Q_{22}]/4 \\ U_2 &= [Q_{11}-Q_{22}]/2 \\ U_3 &= [Q_{11}-2(Q_{12}+2Q_{66})+Q_{22}]/4 \\ U_4 &= [Q_{11}+2(Q_{12}-2Q_{66})+Q_{22}]/4 \\ U_5 &= [Q_{11}-2Q_{12}+Q_{22}]/4 \end{aligned} \tag{14}$$

and the lamination parameters are defined as

$$\zeta_9 = \frac{12}{h^3}\int_{-h/2}^{+h/2} z^2 \cos 2\theta \, dz, \quad \zeta_{10} = \frac{12}{h^3}\int_{-h/2}^{+h/2} z^2 \cos^2 2\theta \, dz,$$

$$\zeta_{11} = \frac{12}{h^3}\int_{-h/2}^{+h/2} z^2 \sin 2\theta \, dz, \quad \zeta_{12} = \frac{12}{h^3}\int_{-h/2}^{+h/2} z^2 \sin 2\theta \cos 2\theta \, dz. \tag{15}$$

The Q_{ij}s in eqn (14) are the reduced ply stiffness coefficients that can be calculated from the engineering constants of the material [Vinson and Sierakowski (1986)]—E_1, E_2, ν_{12} and G_{12} where E_1 is the elastic modulus in the fiber direction, E_2 the modulus in the transverse direction, ν_{12} is the major in-plane Poisson ratio and G_{12} is the shear modulus. It can be shown that $-1 \leqslant \zeta_9 \leqslant 1$ and $\zeta_9^2 \leqslant \zeta_{10} \leqslant 1$ so that, for all laminates, the bending rigidities D_{11}, D_{22}, D_{12} and D_{66} depend only on the two parameters ζ_9 and ζ_{10} which vary in the domain between the parabola $\zeta_{10} = \zeta_9^2$ and the line $\zeta_{10} = 1$ (Fig. 1). Symmetric angle-ply laminates are represented by a point on the parabola PQR. Cross-ply laminates are represented by a point on the line PQ ($\zeta_{10} = 1$). Point P represents unidirectional laminates with fibers oriented at 90° from the x axis. Point Q represents all $\pm 45°$ angle-ply laminates, point R, 0° unidirectional laminates, and point S ($\zeta_9 = 0$, $\zeta_{10} = 0.5$) represents quasi-isotropic lay-ups. The advantages of using this stiffness invariant formulation are that the effect of laminate thickness, lay-up and material properties are separated [eqn (13)], and only four parameters are required to describe all symmetric laminates regardless of the number of plies.

EXACT SOLUTION FOR A SPECIAL CASE

For cross-ply laminates, $D_{16} = D_{26} = 0$ and for laminates with many layers, the effect of these bending–twisting coupling coefficients becomes negligible as the number of plies increases, as we shall verify on numerical examples. For these cases, the governing differential equation obtained by combining eqns (1), (4) and (6) reads

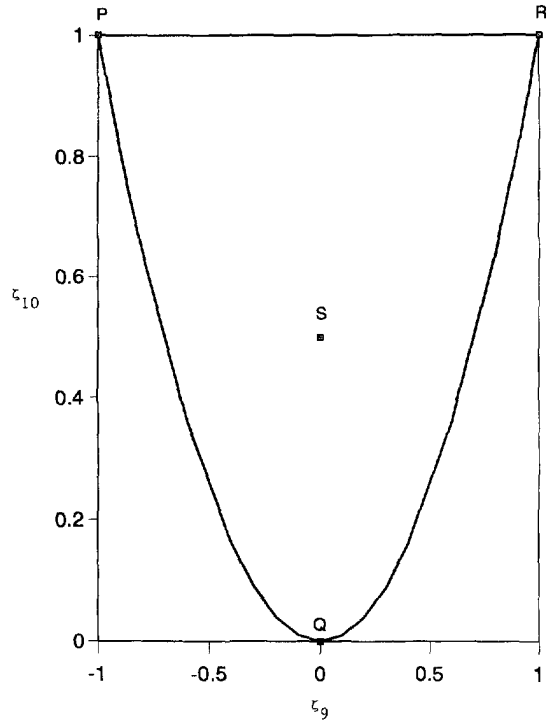

Fig. 1. Lamination parameter space.

$$D_{11}w_{,xxxx}+2(D_{12}+2D_{66})w_{,xxyy}+D_{22}w_{,yyyy}=N_x^o w_{,xx}+N_y^o w_{,yy}+2N_{xy}^o w_{,xy}. \tag{16}$$

For a rectangular plate simply supported along all four edges, the boundary conditions are

$$w(0,y)=w(a,y)=w_{,xx}(0,y)=w_{,xx}(a,y)=0 \tag{17a}$$

$$w(x,0)=w(x,b)=w_{,yy}(x,0)=w_{,yy}(x,b)=0. \tag{17b}$$

For plates with p equal length spans in the x direction, and q equal length spans in the y direction, subjected to biaxial compression ($N_{xy}=0$), the function

$$W_{mn}=\sin\left(\pi\frac{mpx}{a}\right)\sin\left(\pi n\frac{qy}{b}\right) \tag{18}$$

satisfies the governing equation (16) and the boundary conditions (17). The buckling load for mode (m,n) is given exactly by

$$N_x^o=-\frac{\pi^2}{a^2}\frac{D_{11}p^4m^4+2(D_{12}+2D_{66})p^2q^2r^2m^2n^2+D_{22}q^4n^4r^4}{p^2m^2+q^2r^2n^2\,(N_y^o/N_x^o)}. \tag{19}$$

It must be noted that not all buckling loads are obtained using eqn (19), since the solutions to eqns (16) and (17) are not all in the form given by eqn (18). However, when applicable, eqn (19) will be used to check the accuracy of the numerical solutions obtained with the Rayleigh–Ritz method.

RESULTS

In the following examples, the critical buckling load will be non-dimensionalized as $\bar{N}=N_xa^2/D$ where $D=E_1h^3/[12(1-\nu_{12}\nu_{21})]$. Support conditions along the edges of the plate will be denoted by four letters corresponding to the four edges: $x=0$, $y=0$, $x=a$ and

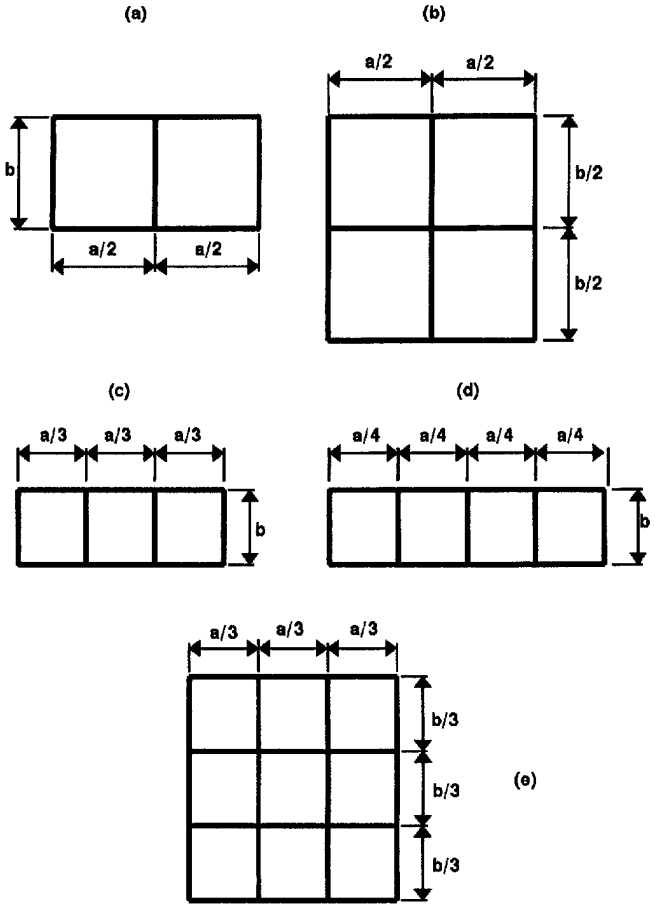

Fig. 2. (a) Two-equal-span plate; (b) two-way two-span plate; (c) three-equal-span plate; (d) four-equal-span plate; (e) two-way three-span plate.

$y = b$. The letters F, S and C denote free, simply supported, and clamped edges respectively. For example, a CSFC plate is clamped along $x = 0$, simply supported along $y = 0$, free along $x = a$, and clamped along $x = b$. Three commonly used material systems are used in this study, and their elastic properties, taken from Tsai (1987), are

$$E_1 = 181\,\text{GPa}, E_2 = 10.35\,\text{GPa}, \nu_{12} = -0.28, G_{12} = 7.17\,\text{GPa}$$

for graphite–epoxy, while

$$E_1 = 38.60\,\text{GPa}, E_2 = 8.27\,\text{GPa}, \nu_{12} = 0.26, G_{12} = 4.14\,\text{GPa}$$

for glass–epoxy, and, for Kevlar–epoxy,

$$E_1 = 76\,\text{GPa}, E_2 = 5.5\,\text{GPa}, \nu_{12} = 0.34, G_{12} = 2.30\,\text{GPa}.$$

Stability of simply supported angle-ply laminated plates with equal length spans

In order to test the accuracy of the model developed and to show the versatility of the approach, the stability of five different plates shown in Fig. 2 will be analyzed. These plates are all simply supported along all four edges and have equal length spans in each direction. The laminates used are assumed to consist of many plies so that bending–twisting coupling effects are negligible ($D_{16} = D_{26} = 0$). For these cases, the exact solution [eqn (19)] can be used to verify the accuracy of the Rayleigh–Ritz model.

Table 1. Buckling loads for a two-equal-span, graphite–epoxy, angle-ply laminated, SSSS plate with many plies under biaxial loading ($N_x = N_y = N$)

θ	Source	$\overline{N_1}$	$\overline{N_2}$	$\overline{N_3}$	$\overline{N_4}$	$\overline{N_5}$	$\overline{N_6}$
	(a) $a/b = 1$						
0	8 × 10	20.8290	21.0734	24.0816	24.6053	29.1758	32.5027
	Exact	20.8290(1,3)	21.0732(1,4)	24.0028(1,5)	24.6053(1,2)	28.8821(1,6)	33.1922(1,1)
15	8 × 11	28.8443	28.8849	31.5516	32.0706	36.3429	43.1962
	Exact	28.8438(1,3)	28.8852(1,2)	31.5514(1,4)	32.0706(1,1)	36.3403(1,5)	42.8428(1,6)
30	8 × 8	28.4582	37.4450	47.1595	50.1709	54.2070	58.0241
	Exact	28.4582(1,1)	37.4451(1,2)	47.1556(1,3)			57.9849(1,4)
45	10 × 8	22.2262	33.6643	41.7250	51.5229	60.4446	63.6969
	Exact	22.2262(1,1)		41.7250(1,2)		60.3426(2,1)	63.6878(1,3)
60	6 × 6	14.496	19.338	31.762	37.446	41.827	44.511
	10 × 8	14.4962	19.2793	30.5049	37.4450	40.3369	41.5882
	Exact	14.4962(1,1)		30.5044(2,1)	37.4451(1,2)		
75	10 × 8	7.8878	10.1173	15.0859	20.0721	28.3320	28.8852
	Exact	7.8878(1,1)		15.0857(2,1)			28.8852(1,2)
90	10 × 8	5.2683	7.0410	10.7996	15.1182	21.0732	22.0870
	Exact	5.2683(1,1)		10.7995(2,1)		21.0732(2,2)	21.7602(3,1)
	(b) $a/b = 2$						
0	8 × 8	21.0732	24.6053	28.8897	32.6480	35.3367	43.2714
	Exact	21.0732(1,2)	24.6053(1,1)	28.8821(1,3)			43.1981(1,4)
15	9 × 9	28.8852	31.5513	42.8429	43.2912	50.3619	51.5325
	Exact	28.8852(1,1)	31.5514(1,2)	42.8428(1,3)			
30	9 × 9	37.4451	54.2071	57.9849	69.0512	85.3702	94.0992
	Exact	37.4451(1,1)		57.9849(1,2)		85.3701(1,3)	
45	9 × 9	41.7250	51.5229	88.9053	88.9053	97.1146	111.010
	Exact	41.7250(1,1)		88.9048(1,2)	88.9048(2,1)		
60	9 × 9	37.4451	41.6549	57.9854	67.2657	86.0963	113.833
	11 × 5	37.4451	41.5880	57.9850	66.7191	85.5491	
	Exact	37.4451(1,1)		57.9849(2,1)		85.3701(3,1)	113.833(1,2)
75	11 × 5	28.8853	29.6977	31.5513	35.8074	42.8915	50.9988
	Exact	28.8852(1,1)		31.5514(2,1)		42.8428(3,1)	
90	11 × 5	21.0732	22.5819	24.6053	26.1843	28.8757	35.9722
	Exact	21.0732(2,1)		24.6053(1,1)		28.8821(3,1)	
	(c) $a/b = 5$						
0	10 × 6	24.0028	32.3215	62.7219	65.7148	88.446	96.0770
	Exact	24.0028(1,1)		62.7200(1,2)		88.444(2,1)	96.0110(2,2)
15	10 × 6	36.3402	45.2688	83.4020	87.7109	113.878	145.364
	Exact	36.3403(1,1)		83.4002(1,2)		113.8765(2,1)	
30	10 × 6	70.6005	79.7018	168.582	168.851	174.750	197.754
	Exact	70.6005(1,1)		168.578(1,2)	168.849(2,1)		
45	11 × 5	118.711	125.796	209.613	229.295	314.889	353.865
	Exact	118.711(1,1)		209.613(2,1)		313.908(3,1)	352.792(1,2)
60	12 × 6	168.334	171.504	210.735	219.302	257.687	272.404
	Exact	168.334(1,1)		210.735(2,1)		257.799(3,1)	
75	16 × 5	178.040	179.439	183.091	186.093	186.424	
	Exact	178.037(3,1)		182.446(4,1)		186.425(2,1)	197.196(5,1)
90	16 × 5	129.831	132.431	139.289	140.677	151.599	170.257
	Exact	128.800(4,1)	131.708(5,1)		140.667(3,1)	145.277(6,1)	167.033(7,1)

The first six buckling loads for a two-equal-span ($p = 2$, $q = 1$), angle-ply laminated, graphite–epoxy SSSS plate [Fig. 2(a)] with an aspect ratio $a/b = 1$ and subjected to biaxial loading ($N_x = N_y = N$) are given in Table 1(a). Numbers in parentheses below the exact values of the critical loads are the values of m and n used in eqn (19). Good agreement is observed between the numerical solution and the exact solution given by eqn (19) for laminates with many plies. For fiber orientation angles of 0° and 15°, the first six critical loads can be determined using the exact solution. For other lay-ups, other modes are present [Table 1(a)]. Figure 3 shows the complex interaction between the first six buckling modes. The lowest buckling load corresponds to the (1,3) mode for small orientation angles; it then switches to the (1,2) mode and then to the (1,1) mode from $\theta = 19.35°$ to 90°. The maximum buckling load for a square SSSS, symmetric angle-ply laminated plate with many plies occurs for $\theta = 19.35°$ when modes (1,1) and (1,2) have the same critical load (Fig. 3). For an aspect ratio $a/b = 2$, the first mode is the (1,2) mode for small orientation angles

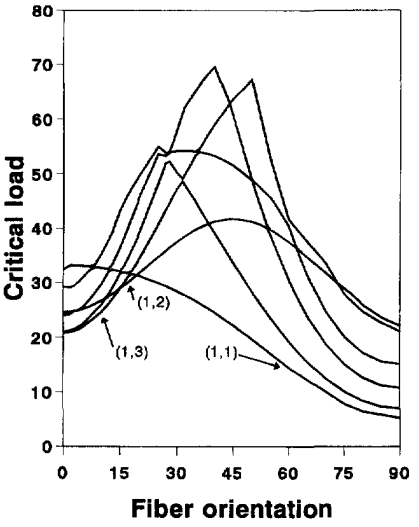

Fig. 3. The first six buckling loads of an SSSS two-equal-span graphite–epoxy plate with many plies subjected to biaxial loading ($N_x = N_y$, $a/b = 1$).

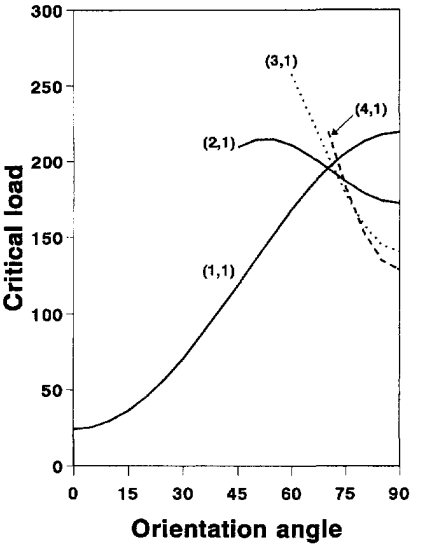

Fig. 4. The lowest buckling load of an SSSS two-equal-span graphite–epoxy plate (many plies, $a/b = 5$) corresponds to one of four modes depending on fiber orientation.

[Table 1(b)]. It then switches to the (1,1) mode and then to the (2,1) mode for large values of θ. It must be noted that, in this case, the buckling loads corresponding to the (1,1) mode are symmetric with respect to $\theta = 45°$. That is, the same loads are obtained for $45° + \alpha$ and $45° - \alpha$. The maximum for the first buckling load is obtained with $\pm 45°$ symmetric angle-ply laminates. For an aspect ratio of 5, the lowest buckling load for symmetric angle-ply laminates switches from mode (1,1) to modes (2,1), (3,1) and (4,1) as the fiber orientation increases (Fig. 4). The lowest buckling load is maximum when the fiber orientation is 70°, and, in that case modes (1,1) and (2,1) have the same critical load. Excellent agreement between the Rayleigh–Ritz and the exact solutions is obtained for the modes predicted by eqn (19) [Table 1(c)]. Table 2(a) gives the first six buckling loads for a two-equal-span square plate under uniaxial compression as a function of the fiber orientation angle. The lowest buckling load is maximum when $\theta = 0°$. In this case, mode (1,1) gives the lowest buckling load for all fiber orientations.

Next, consider two-way two-span ($p = q = 2$), SSSS plates [Fig. 2(b)] with a symmetric angle-ply lay-up and subjected to uniaxial compression ($N_x = N$, $N_y = N_{xy} = 0$). For a plate aspect ratio $a/b = 2$, Table 2(b) shows good agreement between the buckling loads predicted

Table 2. Buckling of a two-equal-span, graphite–epoxy, angle-ply laminated, SSSS plate with many plies under uniaxial compression ($N_x = N$, $N_y = N_{xy} = 0$)

θ	Source	$\overline{N_1}$	$\overline{N_2}$	$\overline{N_3}$	$\overline{N_4}$	$\overline{N_5}$	$\overline{N_6}$
	(a) $a/b = 1$						
0	10×8	41.4902	49.2106	67.7010	82.7743	90.0982	105.477
	Exact	41.4902(1,1)	49.2106(1,2)	67.6944(1,3)			105.369(1,4)
15	10×8	40.0883	57.7705	76.5191	93.7476	93.7459	127.690
	Exact	40.0883(1,1)	57.7705(1,2)		93.7425(1,3)		
30	10×6	35.5727	60.3652	74.8704	98.7684	106.586	142.294
	Exact	35.5727(1,1)		74.8901(1,2)		106.584(1,3)	
45	10×6	27.7827	40.5115	64.1154	83.4506	89.3822	93.8774
	Exact	27.783(1,1)		64.1140(2,1)	83.4500(1,2)		
60	11×6	18.1203	23.2103	32.4109	42.9858	57.9297	72.4816
	Exact	18.1203(1,1)		32.4109(2,1)		57.8779(3,1)	72.4811(2,2)
75	11×6	9.8598	12.1525	16.0285	21.4297	28.7510	37.8238
	Exact	9.8598(1,1)		16.0285(2,1)		28.7293(3,1)	
90	11×6	6.5854	8.4424	11.4745	16.1639	22.3796	26.3414
	Exact	6.5854(1,1)		11.4745(2,1)		22.3646(3,1)	26.3415(2,2)
	(b) $a/b = 2$						
0	10×6	105.367	139.570	166.858	188.248	196.847	216.933
	Exact	105.366(1,1)				196.843(2,1)	
15	10×6	157.758	185.839	231.086	238.868	250.472	263.665
	Exact	157.757(1,1)		231.082(2,1)			
30	10×6	289.928	294.824	299.564	353.871	368.483	390.933
	Exact	289.925(1,1)		299.561(2,1)			
45	10×6	333.803	345.455	369.660	396.920	444.532	451.0
	Exact	333.800(2,1)		367.974(3,1)		444.524(4,1),	
60	14×6	272.472	277.780	292.36	298.557	299.558	311.
	Exact	272.455(3,1)		289.925(4,1)		299.561(2,1)	
75	15×5	159.295	163.303	166.541	167.954		
	Exact	157.757(4,1)		166.653(3,1)	168.619(5,1)	190.412(6,1)	
90	15×5	106.952	110.679	118.141	120.330		
	Exact	105.366(4,1)		111.3728(5,1)	120.346(3,1)	128.365(6,1)	152.915(7,1)

by the Rayleigh–Ritz model and the exact solution for laminates with many plies. The lowest buckling load corresponds to the (1,1) mode for fiber orientation angles lower than 31°, followed by the (2,1) mode between 31° and 52°, the (3,1) mode between 52° and 70°, and the (4,1) mode beyond that (Fig. 5). Mode (2,1) gives a curve that is symmetric about $\theta = 45°$ and angle ply laminates with a $\pm 45°$ lay-up will have the highest buckling load. The curves for modes (1,1) and (4,1) are mirror images of each other about the $\theta = 45°$ line. For a square plate ($a/b = 1$), the maximum buckling load occurs for $\theta = 45°$ which corresponds to the (1,1) mode as shown in Fig. 6. For two-way two-span square plates, subjected to biaxial compression ($N_x = N_y$), only the 0–45° range of fiber orientations need be examined (Table 3) because of the symmetry of the geometry and the loading. The lowest buckling load corresponds to the (1,1) mode, and the optimum occurs at 45°.

For three equal-span ($p = 3$, $q = 1$) SSSS plates [Fig. 2(c)] ($a/b = 3$) subjected to uniaxial compression ($N_y = N_{xy} = 0$), the first buckling load is maximum when $\theta = 45°$ [Table 4(a)]. When the same plate is subjected to biaxial loading, the maximum also occurs for $\theta = 45°$ [Table 4(b)].

For four equal-span ($p = 4$, $q = 1$) plates [Fig. 2(d)] simply supported along all edges ($a/b = 4$) and subjected to uniaxial compression, the first buckling load is maximum when $\theta = 45°$ (Fig. 7). The lowest buckling load is given by mode (1,1) when $\theta \leqslant 58°$ and mode (2,1) for $\theta > 58°$. Agreement between the Rayleigh–Ritz solution and the exact solution is good, but a large number of terms is needed in the x direction for convergence (Table 5).

For a two-way three-span ($p = q = 3$) SSSS plate [Fig. 2(e)] subjected to uniaxial compression, the Rayleigh–Ritz solution is in good agreement with the exact solution (Table 6). The lowest buckling load is obtained for a fiber orientation angle of 45° for mode (1,1).

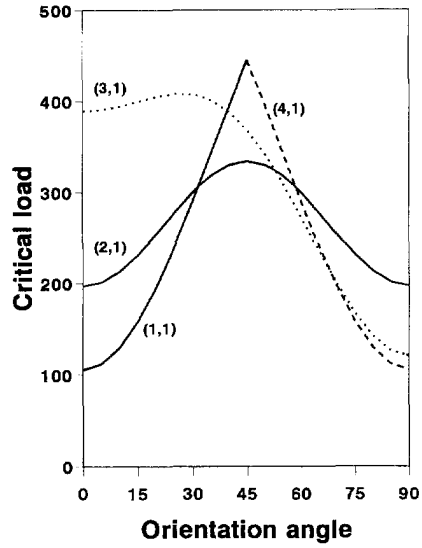

Fig. 5. Lowest buckling load for a two-way two-span SSSS graphite–epoxy plate (many plies, $a/b = 2$) under uniaxial compression.

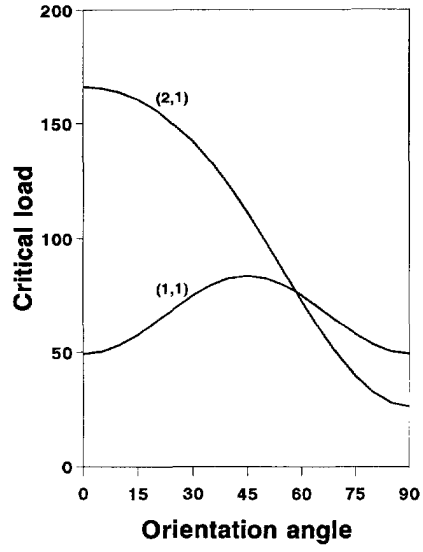

Fig. 6. Lowest buckling load for a two-way two-span SSSS graphite-epoxy plate (many plies, $a/b = 1$) under uniaxial compression.

Table 3. Buckling loads of two-way two-span, graphite–epoxy, square SSSS plates with many plies under biaxial compression ($N_x = N_y = N$)

θ	Source	$\overline{N_1}$	$\overline{N_2}$	$\overline{N_3}$	$\overline{N_4}$	$\overline{N_5}$	$\overline{N_6}$
0	7×10	21.0735	22.5820	24.6053	26.1843	29.1756	33.0063
	Exact	21.0732(1,2)		24.6053(1,1)		28.8821(1,3)	
15	7×10	28.9214	29.6977	31.5515	35.8074	43.2326	43.8365
	Exact	28.8852(1,1)		31.5514(1,2)		42.8428(1,3)	
30	8×8	37.4451	41.6549	54.2071	57.4283	58.0241	
	Exact	37.4451(1,1)			57.985(1,2)		
45	8×8	41.7250	51.5229	51.5229	60.6226	88.9981	88.9981
	Exact	41.7250(1,1)				88.9048(1,2)	88.9048(2,1)

Table 4. Buckling loads for three equal-span, graphite–epoxy, angle-ply laminated SSSS plates with many plies ($a/b = 3$)

θ	Source	$\overline{N_1}$	$\overline{N_2}$	$\overline{N_3}$	$\overline{N_4}$	$\overline{N_5}$	$\overline{N_6}$
			(a) uniaxial compression ($N_x = N$, $N_{xy} = N_y = 0$)				
0	10×6	110.724	155.499	237.077	257.962	274.386	360.266
	Exact	110.724(1,1)		237.074(1,2)			
15	10×6	129.984	169.369	259.520	354.957	361.681	385.631
	Exact	129.984(1,1)			354.953(1,2)	360.795(2,1)	
30	10×6	168.503	194.616	254.616	320.779	402.681	523.698
	Exact	168.503(1,1)			320.154(2,1)		
45	10×6	187.762	199.140	225.316	250.342	294.921	353.112
	Exact	187.762(1,1)			250.045(2,1)		
60	9×4	163.676	165.086	168.538	169.104	191.289	223.650
	Exact	163.083(2,1)		168.503(1,1)			213.650(3,1)
75	10×5	81.037	89.678	92.081	123.181	126.708	129.983
	Exact		88.738(2,1)		107.107(3,1)		129.984(1,1)
90	9×5	59.487	61.691	77.039	89.830	105.50	108.26
	Exact	59.268(2,1)		72.205(3,1)		103.271(4,1)	
			(b) biaxial compression ($N_x = N_y = N$, $N_{xy} = 0$)				
0	10×8	47.415	55.362	59.404	65.002	71.708	
	Exact	47.415(1,2)	55.3620(1,1)		64.9847(1,3)		
15	8×6	64.9919	70.9911	83.6809	89.0703	97.6904	106.193
	Exact	64.9918(1,1)	70.9906(1,2)			96.3963(1,3)	
30	8×6	84.2515	102.320	130.467	143.406	152.001	180.062
	Exact	84.2514(1,1)		130.466(1,2)			
45	8×4	93.8901	104.700	134.001	200.75	201.535	211.141
	Exact	93.8812(1,1)			200.036(1,2) (2,1)		
60	10×6	84.2481	87.1519	88.8339	99.8667	130.739	143.294
	Exact	84.2514(1,1)				130.466(2,1)	
75	10×6	64.9918	65.8426	68.1758	71.0426	78.1601	91.2346
	Exact	64.992(1,1)			70.991(2,1)		
90	12×4	47.4193	48.8289	52.2309	55.2342	55.3553	59.2158
	Exact	47.415(2,1)			55.362(1,1)		

These five examples show the versatility of the Rayleigh–Ritz formulation developed here since plates with arbitrary numbers of line supports can be analyzed. For SSSS plates with equal length spans, many of the critical loads can be predicted using eqn (19) and the Rayleigh–Ritz approach gives very accurate results using reasonable numbers of terms in

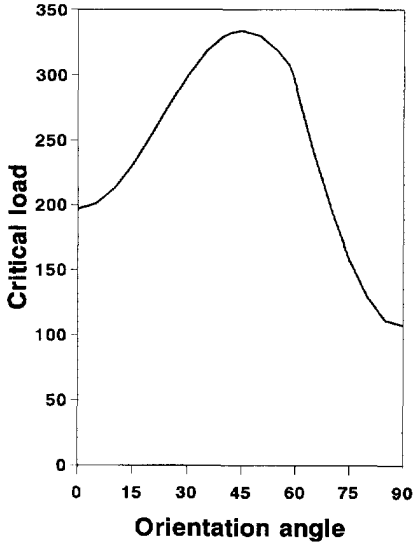

Fig. 7. Lowest buckling load for four equal spans SSSS graphite–epoxy plates (many plies, $a/b = 4$) under uniaxial compression.

Table 5. Buckling loads of four equal-span, graphite–epoxy, angle-ply laminated SSSS plates with many layers in uniaxial compression ($a/b = 4$, $N_{xy} = N_y = 0$)

θ	Source	$\overline{N_1}$	$\overline{N_2}$	$\overline{N_3}$	$\overline{N_4}$	$\overline{N_5}$	$\overline{N_6}$
0	10×6	196.843	243.317	360.527	421.470	460.062	519.255
	Exact	196.843(1,1)			421.464(1,2)		
15	10×6	231.082	271.957	375.074	514.569	631.034	
	Exact	231.082(1,1)				631.027(1,2)	641.413(2,1)
30	16×5	299.561	326.631	395.034	460.883	567.593	611.
	Exact	299.561(1,1)				569.164(2,1)	
45	14×6	333.800	345.560	375.741	413.812	454.281	576.862
	Exact	333.800(1,1)				444.524(2,1)	
60	16×4	290.598	292.832	299.561	300.003	301.068	341.895
	Exact	289.925(2,1)		299.561(1,1)			
75	16×4	158.655	163.437	182.141	215.783	222.480	227.239
	Exact	157.757(2,1)		190.412(3,1)			
90	16×4	106.081	110.314	123.558	167.120	179.195	190.694
	Exact	105.366(2,1)		128.365(3,1)		183.592(4,1)	

Table 6. Buckling of a two-way three-span graphite epoxy plate with many plies under uniaxial compression (SSSS, $a/b = 1$, $N_y = N_{xy} = 0$)

θ	Source	$\overline{N_1}$	$\overline{N_2}$	$\overline{N_3}$	$\overline{N_4}$	$\overline{N_5}$	$\overline{N_6}$
0	8×6	110.727	115.923	147.221	155.555	160.415	189.752
	Exact	110.724(1,1)					
15	8×6	129.988	138.770	169.417	177.809	192.483	229.160
	Exact	129.984(1,1)					
30	8×6	168.511	187.242	194.640	212.599	255.605	271.689
	Exact	168.511(1,1)					
45	10×6	187.779	199.155	220.474	225.328	229.720	250.500
	Exact	187.762(1,1)					250.500(2,1)
60	8×6	163.670	167.199	168.584	169.042	183.892	194.208
	Exact	163.083(2,1)		168.503(1,1)			
75	8×6	89.0271	95.7761	107.170	111.771	112.375	125.097
	Exact	88.7381(2,1)		107.107(3,1)			
90	12×6	59.3054	61.2357	68.4071	71.9996	76.1165	77.2961
	Exact	59.2684(2,1)			72.2052(3,1)		

the displacement approximation. As the fiber orientation is changed, the lowest critical buckling load does not always correspond to the same mode shape.

Effect of lamination and material properties

In the examples studied above, the laminates are always assumed to contain many plies so that the bending–twisting coupling effects are negligible. To determine the effect of the number of plies on the lowest buckling load, consider a two-equal-span ($p = 2, q = 1$), SSSS graphite–epoxy plate subjected to biaxial loading ($N_x = N_y$). Results for uniaxial, $[\theta, -\theta]_s$, $[\theta, -\theta, \theta]_s$ laminates and laminates with many plies are compared in Fig. 8. It is shown that, while the bending–twisting coupling effects are significant for laminates with few plies, they become negligible when the number of plies becomes larger than six.

Previous examples considered only symmetric angle-ply laminates and generally the optimal design happens to be an angle-ply laminate. Here, the more general case of two-span ($p = 2$, $q = 1$), SSSS, graphite–epoxy, symmetrically laminated plates ($a/b = 2.5$) under biaxial loading are studied. The lowest buckling load is given by the (1,1) mode over the entire domain in the ζ_9–ζ_{10} plane. Isocurves for that mode are straight parallel lines [(Fig. 9(a)]. For a given mode shape (fixed values of m and n), eqn (19) indicates that the critical load is a linear function of ζ_9 and ζ_{10} since, from eqn (13), the bending rigidities D_{11}, D_{22}, D_{12} and D_{66} are linear functions of the lamination parameters ζ_9 and ζ_{10}. The surface $N = N(\zeta_9, \zeta_{10})$ is a plane, the contour lines in Fig. 9(a) should be straight and equally spaced, and the maximum should occur for a point on the parabola (angle-ply laminate). The optimum lay-up for a two-equal-span, SSSS plate with $a/b = 2.5$ is a symmetric angle ply laminate with $\theta = 54.4°$. For $a/b = 1$, the variation of the lowest buckling load [Fig.

Table 7. Buckling of a two-way two-span, graphite–epoxy, SSSS plate with many plies under uniaxial compression ($a/b = 0.75$, $N_y = N_{xy} = 0$)

θ	Source	$\overline{N_1}$	$\overline{N_2}$	$\overline{N_3}$	$\overline{N_4}$	$\overline{N_5}$	$\overline{N_6}$
	(a) $a/b = 0.75$						
0	8 × 8	44.4000	46.1809	67.7327	78.9204	85.6027	87.1717
	Exact	44.3999(1,1)		67.6944(1,2)			
15	8 × 6	47.1004	50.6437	83.4295	86.7092	95.7386	123.109
	Exact	47.1003(1,1)				93.7425(1,2)	
30	10 × 8	51.2530	57.8223	75.7998	81.8425	121.289	125.721
	Exact	51.2530(1,1)				121.286(2,1)	
45	10 × 8	49.2954	60.6405	61.4258	71.5081	83.2853	89.7902
	Exact	49.2954(1,1)				83.2839(1,2), (2,1)	
60	10 × 8	38.5273	42.3587	48.2956	54.2886	54.8991	55.2710
	Exact	38.5272(1,1)	48.2950(2,1)				
75	10 × 8	24.5930	24.8722	25.0581	30.8776	31.2083	33.7792
	Exact	24.5920(2,1)		25.0587(1,1)			
90	10 × 8	16.3200	17.4634	18.9484	21.7276	22.4646	23.9452
	Exact	16.3197(2,1)		18.9485(1,1)			
	(b) $a/b = 1$						
0	10 × 6	49.2108	54.2322	90.0984	94.4553	109.065	142.611
	Exact	49.2106(1,1)				105.366(1,2)	
15	8 × 6	57.7706	65.9157	93.7607	101.097	160.655	162.928
	Exact	57.7705(1,1)				157.757(1,2)	160.3532(2,1)
30	10 × 6	74.8904	92.1203	98.7684	114.371	142.294	153.084
	Exact	74.8901(1,1)				142.291(2,1)	
45	10 × 6	83.4506	93.8774	111.133	114.575	120.327	127.429
	Exact	83.4500(1,1)		111.131(2,1)			
60	10 × 6	72.4820	73.7198	74.8911	85.2946	90.9995	95.9602
	Exact	72.4811(2,1)		74.8901(1,1)			94.8556(3,1)
75	10 × 6	39.4398	42.0242	47.9637	52.6551	56	57
	Exact	39.4392(2,1)		47.6031(3,1)			57.7705(1,1)
90	10 × 4	26.4340	28.4626	32.4411	37.7175	42.4857	44.2763
	Exact	26.3415(2,1)		32.0912(3,1)			

9(b)] with the two lamination parameters is similar over most of the domain where straight isocurves are associated with mode (1,1). However, in the upper right corner, the lowest critical load corresponds to the (1,3) mode, and, therefore, the $N = N(\zeta_9, \zeta_{10})$ surface consists of two planar surfaces corresponding to the (1,1) and (1,3) modes, which again indicates that the maximum occurs on the boundary of the domain and that the optimal

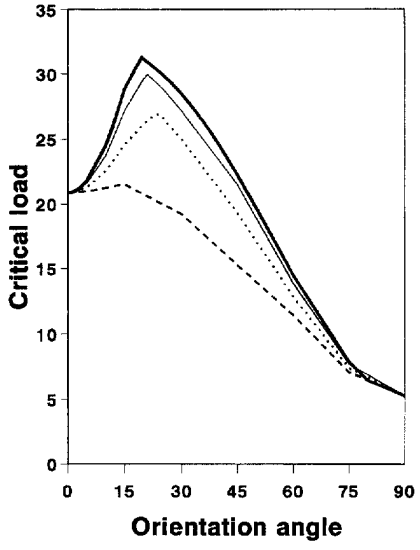

Fig. 8. Lowest buckling of two equal span SSSS graphite–epoxy ($N_x = N_y$, $a/b = 1$) as a function of the number of plies (heavy line: many plies, thin line: 6 plies, dotted line: 4 plies, dashed line: 1 ply).

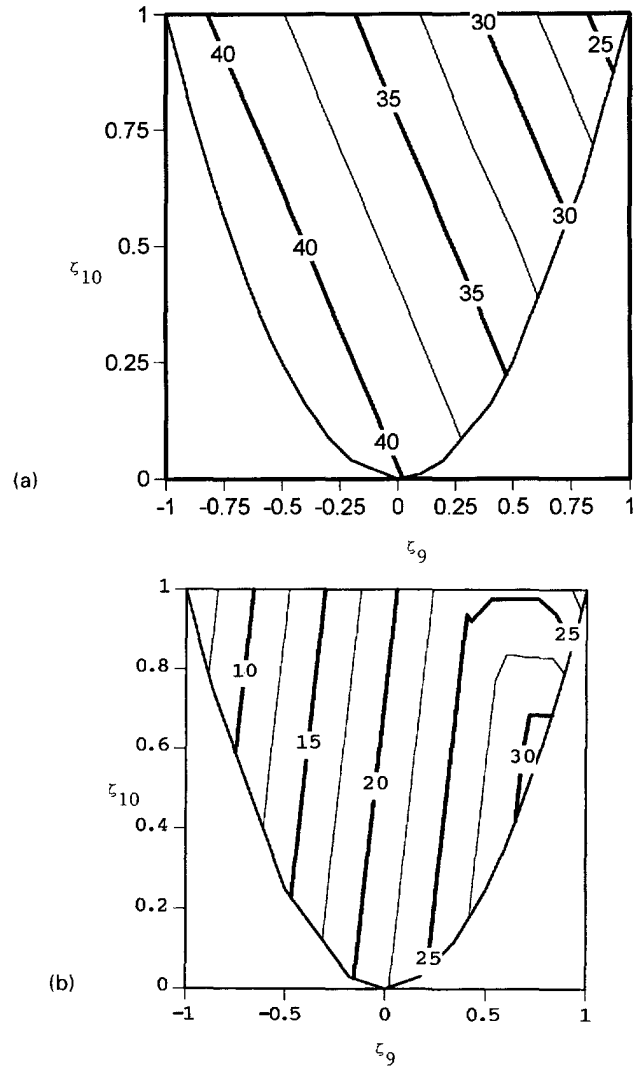

Fig. 9. Lowest critical load for a two-span SSSS graphite–epoxy plate with many plies subjected to biaxial compression ($N_x = N_y$): (a) $a/b = 2.5$, (b) $a/b = 1.0$.

layup is again an angle-ply laminate. The optimum lamination scheme for a square two-equal-span SSSS plate under biaxial compression is an angle-ply laminate with $\theta = 19.5°$.

The effect of the plate aspect ratio a/b on the optimum fiber orientation, for two equal-span (p = 2, q = 1), SSSS plates with many plies subjected to biaxial loading is shown in Fig. 10. In addition to graphite–epoxy, E glass–epoxy and Kevlar–epoxy are also considered. For this case, the optimum fiber orientation is $\theta = 45°$ when $a/b = 2$ for all material systems, and the lowest buckling load corresponds to the (1,1) mode for moderate values of the ratio a/b. When a/b is small, the optimum fiber orientation is found when modes (1,1) and (1,2) have the same critical load. For large aspect ratios, modes (1,1) and (2,1) have the same critical load for the optimal fiber orientation. When a/b becomes large, the optimum fiber orientation remains nearly constant in all cases (Fig. 10). Results for graphite–epoxy and Kevlar–epoxy remain very close over the whole range and would not be distinguishable in Fig. 10.

CCSS three-unequal-span plate

To illustrate the versatility of the approach developed here for studying rectangular plates with arbitrary boundary conditions and line supports located arbitrarily, a plate clamped along the $x = 0$ and $y = 0$ edges and simply supported along the other two edges is considered. Line supports are located at $x = a/4$ and $x = 3a/4$, and plates with aspect

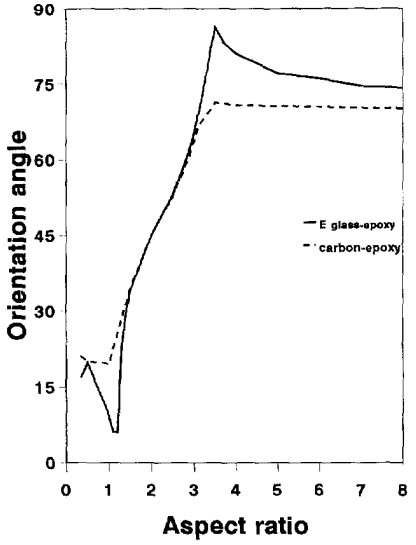

Fig. 10. Effect of material properties on the lowest buckling load of two-span SSSS plates with many plies subjected to biaxial compression.

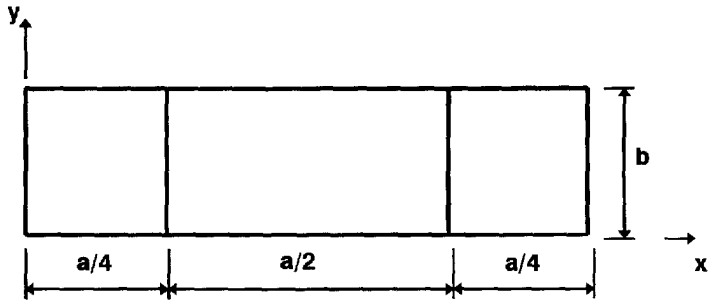

Fig. 11. Three-unequal-span plate.

ratios $a/b = 4$ are analyzed (Fig. 11). The lowest buckling load for symmetric angle-ply laminates is shown in Fig. 11 as a function of fiber orientation. The maximum occurs for $\theta = 64^\circ$. Considering all symmetric laminates with many plies, the optimum design is still $a \pm 64^\circ$ angle ply laminate as shown in Fig. 12. Over most of the range, the lowest buckling mode is the (1,1) mode, and the isocurves are nearly vertical (Fig. 12). In the upper left corner, modes (2,1) and (3,1) are present, and the isocurves become curved. However, the maximum buckling load still occurs on the boundary $\zeta_{10} = \zeta_{01}^2$, and the optimum lay-up is a symmetric angle-ply laminate with $\theta = 64^\circ$.

SSSS plate with point support in the center

Point supports can easily be introduced using the Lagrange multiplier technique (Reddy, 1984). For a rectangular ($a/b = 2$) graphite–epoxy symmetrically laminated SSSS plate, the first three critical loads for angle-ply lay-ups vary with fiber orientation as shown in Fig. 13. The optimal fiber orientation for rectangular SSSS graphite–epoxy plates with a point support in the center is given in Fig. 14 as a function of the aspect ratio a/b. Because the plate is simply supported along all four edges and the support is located in the center, only aspect ratios larger than 1 need be investigated, and values for $a/b < 1$ can be deduced from these results. The optimum fiber orientation remains equal to $\pm 45^\circ$ for $1 \leqslant a/b \leqslant 2$ and then increases to $\pm 71^\circ$ for $a/b = 3.5$ for higher aspect ratios. The optimum fiber orientation angle is $\theta = 70^\circ$ (Fig. 14).

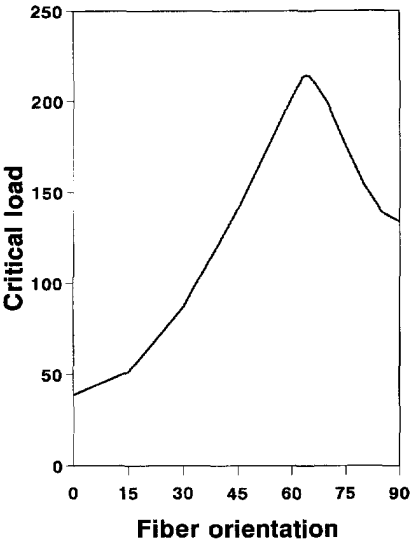

Fig. 12. Lowest buckling load of CCSS three-unequal-span plate with many plies ($a/b = 4$, angle-ply laminates).

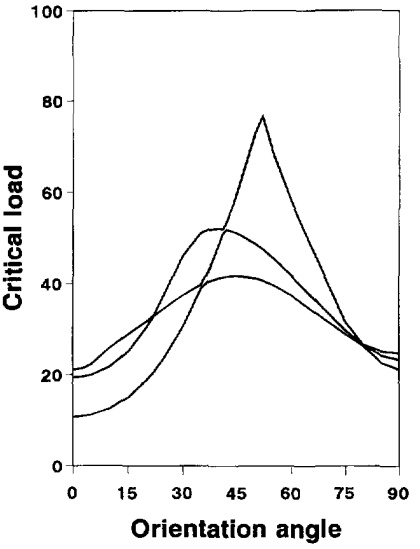

Fig. 13. Lowest buckling load of CCSS three-unequal-span plate with many plies ($a/b = 4$, symmetric laminates).

CONCLUSION

In this article, a general approach has been presented to analyze the stability of rectangular plates with any number of intermediate line supports. Any combination of support conditions along the edges can be considered, and the location of the intermediate supports is arbitrary. Using the Rayleigh–Ritz method with simple polynomial approximation functions, the elastic and geometric stiffness matrices are obtained exactly, and the resulting eigenvalue problem is solved numerically. For symmetric laminates, the plate constitutive equations are written in terms of four non-dimensional lamination parameters. Extensive results are presented for six different plates, and, for several cases, some of the critical loads can be checked using an exact solution. This allowed verification of the Rayleigh–Ritz formulation and its convergence to be studied. Point supports are introduced using the Lagrange multiplier technique.

In general, the bending–twisting coupling terms are negligible for laminates with more than six plies, in which case, only two independent parameters are needed to describe all

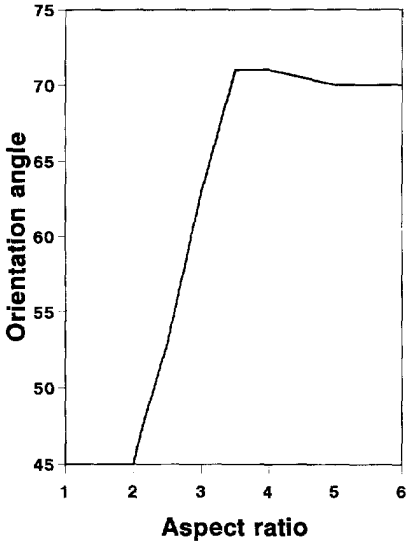

Fig. 14. Optimal fiber orientation for SSSS graphite–epoxy plates with many plies and a point support in the center.

symmetric laminates. For all the cases considered, the optimum lay-up is a symmetric angle-ply laminate and the effect of material properties is shown to be small for common material systems.

REFERENCES

Abrate, S. and Foster, E. (1994). Vibrations of composite plates with intermediate line supports. To appear in *J. Sound Vibr.*

Azimi, S., Hamilton, J. F. and Soedel, W. (1984). The receptance method applied to the free vibration of continuous rectangular plates. *J. Sound Vibr.* **93**(1), 9–29.

Kim, C. S. and Dickinson, S. M. (1987). The flexural vibration of line supported rectangular plate systems. *J. Sound Vibr.* **114**(1), 129–142.

Leissa, A. W. (1987). An overview of composite plate buckling. In *Composite Structures* 4 (Edited by I. M. Marshall), Vol. 1. Elsevier Applied Science, Oxford.

Liew, K. M. and Lam, K. Y. (1991). Vibration analysis of multi-span plates having orthogonal straight edges. *J. Sound Vibr.* **147**(2), 255–264.

Reddy, J. N. (1984). *Energy and Variational Methods in Applied Mechanics*. J. Wiley, New York.

Tsai, S. W. (1987). *Composites Design*. Think Composites, Dayton, OH.

Vinson, J. R. and Sierakowski, R. L. (1986). *The Behavior of Structures Composed of Composite Materials*. Kluwer Academic Publishers, Dordrecht, The Netherlands.